Est. 1984

ORIENTAL JOURNAL OF CHEMISTRY
An International Open Free Access, Peer Reviewed Research Journal

www.orientjchem.org

ISSN: 0970-020 X
CODEN: OJCHEG
2012, Vol. 28, No. (2):
Pg. 815-827

NMR Studies of BH_3-attaching in the Zigzag and Armchair BN Nanotubes: A DFT Study

REZA SOLEYMANI [1]*, MARYAM KARIMI-CHESHMEH ALI [2] and NAHID NIAKAN [3]

[1]Young Researchers Club, Shahre-rey Branch, Islamic Azad University, Tehran (Iran).
[2]Department of Chemistry, Mahshahr Branch, Islamic Azad University, Mahshahr (Iran).
[3]Department of Chemistry, Shahre-rey Branch, Islamic Azad University, Tehran (Iran).
*Corresponding author E-mail: reza.soleymani@hotmail.com

(Received: April 06, 2012; Accepted: May 20, 2012)

ABSTRACT

This article investigates the structure of armchair (*3, 3*) and zigzag (*6, 0*) boron nitrogen nanotubes (BNNTs) affected by addition of a Borane group (BH_3) by performing density functional theory (DFT) calculation at B3LYP levels of theory and 6-31G(d) basis set. The changes of the nuclear magnetic resonance (NMR) parameter of these structures were calculated by GIAO method implemented in the *Gaussian 09W* program of package. The results indicated that the addition of BH_3 to nanotubes affected the values of isotropic chemical shift (CS^I) and anisotropic chemical shift (CS^A) parameters. The addition of BH_3 also affected the values of bond length and bond angle. The results revealed that the attachment of BH_3 group to the surface of nanotubes had the potential to increase the chemical shift of the nuclei directly linked to Borane molecules.

Key words: BNNTs, CS^A, CS^I, DFT, NMR, BN Nanotubes.

INTRODUCTION

Boron nitride compound, with chemical formula BN, is made up of boron and nitrogen atoms [1, 2]. This compound is not found in nature and can only be constructed from boric acid or boron trioxide in laboratory. It has hexagonal or cubic structure. The hexagonal form (h-BN) is among the most stable and softest BN polymorphs and is used as a lubricant or an additive to cosmetic products [3-7]. BNNTs are very similar to carbon nanotubes (CNTs) and, therefore, can form graphite like hexagonal layers. BN is chemically inerter than carbon especially in high temperatures. However, the electronic properties of BNNTs are less adjustable than that of CNTs. BNNTs are also better field emitters than CNTs. BNNTs like nanotubes produced from tungsten and sulfur or tungsten and selenium has less flexibility and elasticity in comparison with CNTs. However, BN nano-mesh has a two dimensional structure which is not only stable to decomposition under vacuum, some gases and some liquids but also resistant to high temperatures of about 900 °C [7-10]. Limitations in production and application of CNTs have triggered a deluge of interest in BNNTs. This material has a

layered structure so that each boron atom is bonded to a nitrogen atom. This material has specific properties such as having superior mechanical properties (young's modulus 1.18 TPa) and high heat resistance and remaining semi-conductive. This material is employed in production of fiber. BNNTs fibers are utilized in production of commercial textile, military uniforms, and solar cells [10-16]. Many theoretical and experimental researches were conducted to study the synthesis of BNNTs. This material was theoretically predicted in 1994 but its synthesis was experimentally realized in 1995 in laboratory with arc-charging method using BN electrode. Later, other methods such as arc-melting, high temperature chemical reaction, carbon nanotube templates, and laser ablating were reported for synthesis of this material [16-22]. Recently, Zeng *et al.* has investigated the effect of NH_3 on these nanotubes [23]. Zahedi *et al.* has also conducted theoretical researches on (*10, 0*) nanotubes investigating the effect of NH_3 on NMR parameters of these structures [24]. Here, regarding the wide application and great importance of this material, armchair and zigzag BNNTs were studied to investigate how their properties would be affected by addition of a BH_3 group. For this reason, NMR dependant parameters such as CS^I and CS^A were calculated. Finally, some of their structural parameters were evaluated.

Computational Details

All the computations were carried out by performing DFT calculation at B3LYP and 6-31G(d) levels using the *Gaussian 09W* program of package [25]. This was performed on a personal computer (Pentium® 4 CPU 1.70 GHz and 4.00 GB of RAM) with Microsoft Windows 7 system. All the calculations were carried out in gas phase at atmospheric pressure and a temperature of 298 K. NMR parameters were calculated by GIAO method [26, 27]. The armchair (*3, 3*) and zigzag (*6,* 0) models of BNNTs were designed using *Gauss View* and optimized through semi-empirical method Austin Model 1 (AM1) [28]. Each nanotube had a length of 10 Å. The values of CS^I and CS^A parameters were determined through relations 1 and 2 [29-31]. CS tensors in the principal axes system (PAS) ($\sigma_{33} > \sigma_{22} > \sigma_{11}$)

$$CS^I (ppm) = (\sigma_{11} + \sigma_{22} + \sigma_{33})/3 \quad ...(1)$$

$$CS^A (ppm) = \sigma_{33} - (\sigma_{11} + \sigma_{22})/2 \quad ...(2)$$

RESULTS AND DISCUSSION

After the final optimization of the structure of nanotubes the values of chemical shifts and structural parameters were evaluated. In order to do so, the structural parameters of armchair (*3, 3*) and zigzag (*6, 0*) models of BNNTs were investigated under perfect and BH_3 attached states.

Geometrical parameter

Bond length and angle are considered as the main structural parameters. In this article, bond lengths, expressed in angstrom unit, and bond and dihedral angles, specified in degrees, were determined and the effect of adding a BH_3 group to the surface of BNNTs was investigated (Fig 1-5).

Bond length in (3, 3) armchair BNNTs

The results of armchair (*3, 3*) BNNTs indicated that addition of BH_3 group induced changes in the bond length in proportion with the position which BH_3 took on the ring. Accordingly, all bond lengths would change by addition of BH_3 groups and the changes would be bigger in bonds which were closer to the BH_3 bonding area. For example, N2-B55 direct bond induced the attachment of a BH_3 group to the surface of the nanotube. The biggest changes in bond length were observed in N2-B36 bond (1.458 Å to 1.496 Å), N2-B47 bond (1.465 Å to 1.504 Å), and N2B52 (1.453 Å to 1.509 Å). Other bond lengths were also subjected to similar changes but their changes were smaller (Table 1).

Bond length in (6, 0) zigzag BNNTs

The results of zigzag (*6,* 0) BNNTs were completely similar to the results of armchair (*3, 3*) BNNTs. Similarly, the biggest changes were observed in bonds which were closer to the BH_3 group. In this form, N19-B61 direct bond induced the attachment of a BH_3 group to the surface of the nanotube. This factor also resulted in bigger changes in the bonds which contained N19 atom. For example, the biggest changes in bond length were observed in N19-B42 bond (1.458 Å to 1.506 Å), N19-B47 bond (1.457 Å to 1.507 Å), and N19B55 bond (1.450 Å to 1.543 Å). No significant change was observed in other bond lengths (Table 2).

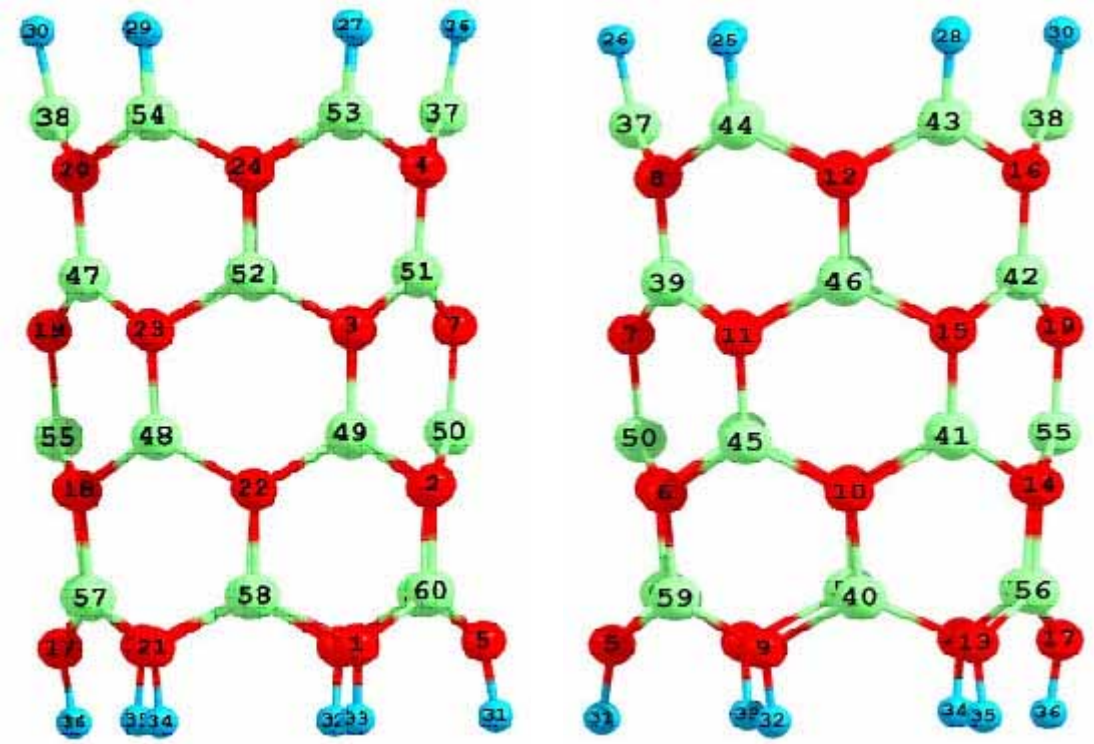

Fig. 1: 2D views of the perfect in (6, 0) zigzag model of BNNTs

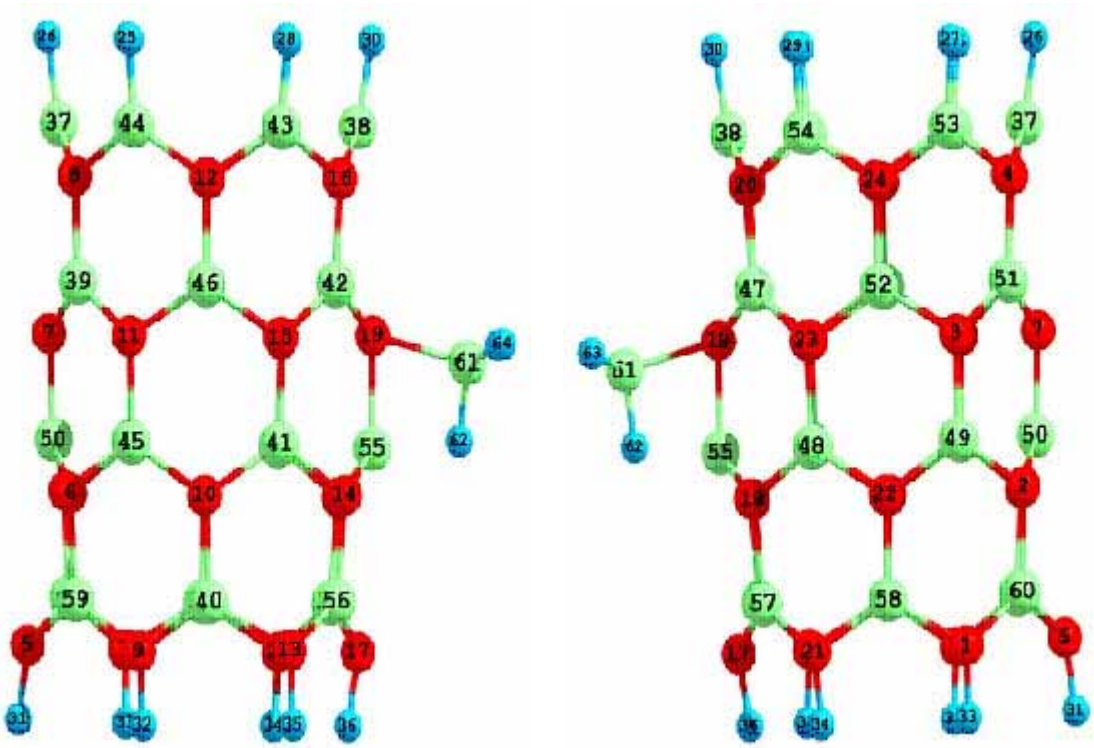

Fig. 2: 2D views of the BH_3-attach in (6, 0) zigzag model of BNNTs

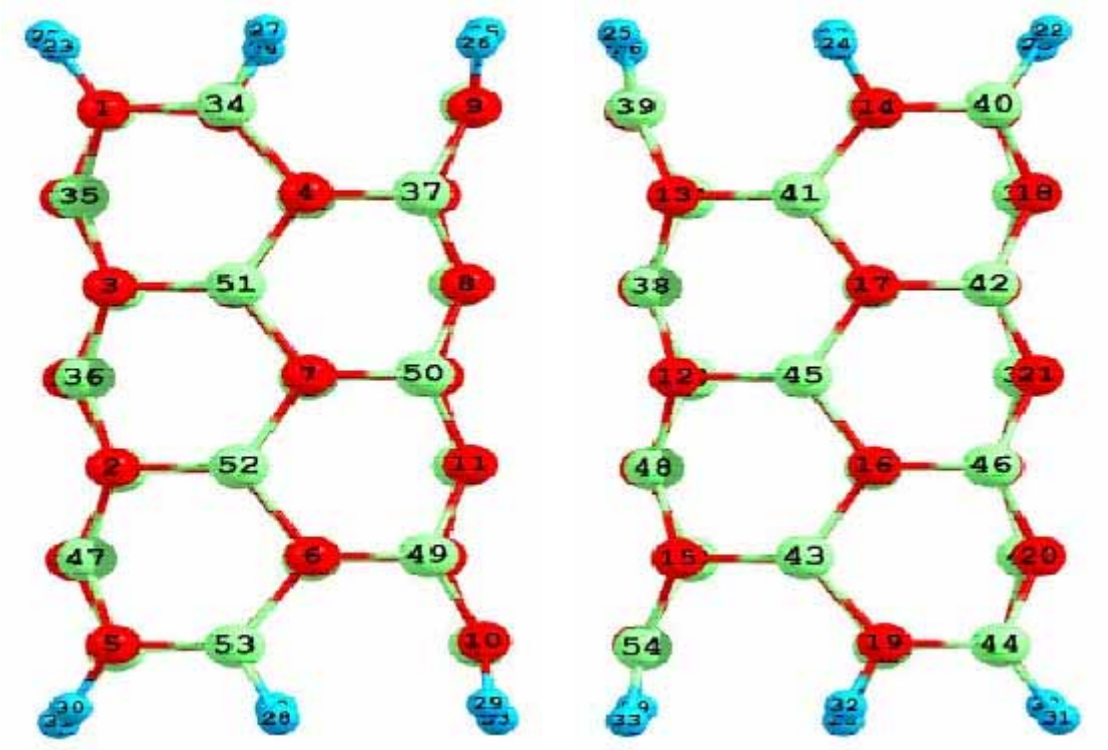

Fig. 3: 2D views of the perfect in (3, 3) armchair model of BNNTs

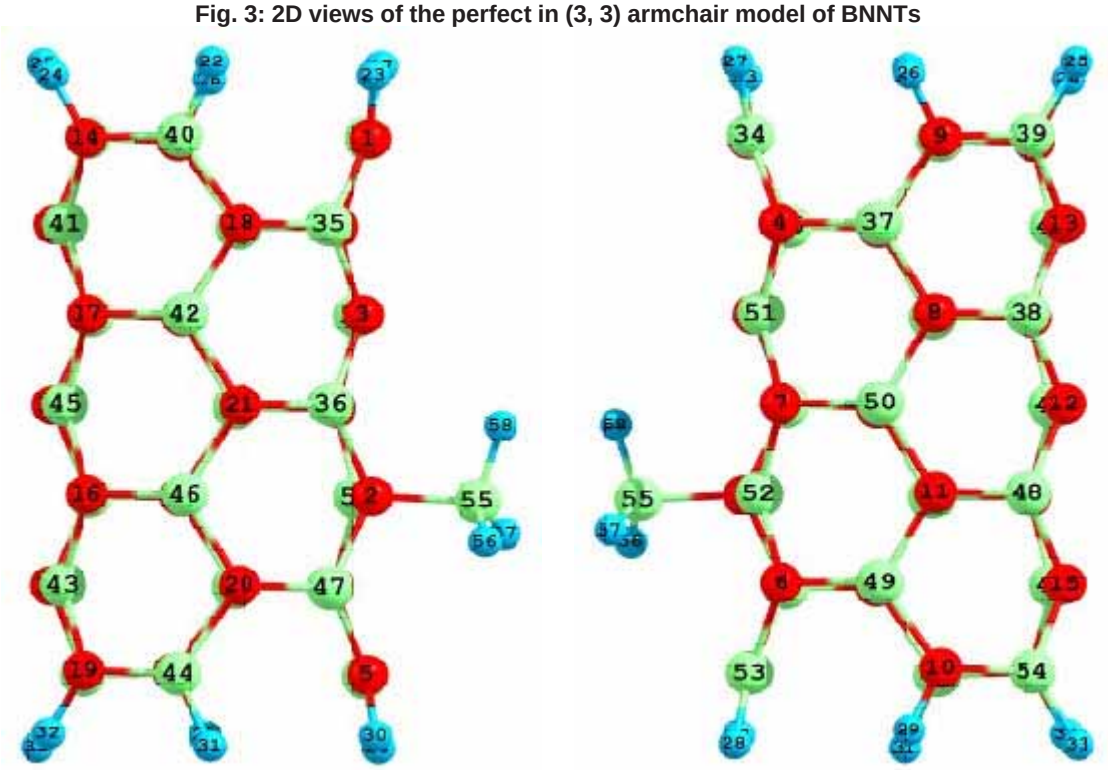

Fig. 4: 2D views of the BH_3-attach in (3, 3) armchair model of BNNTs

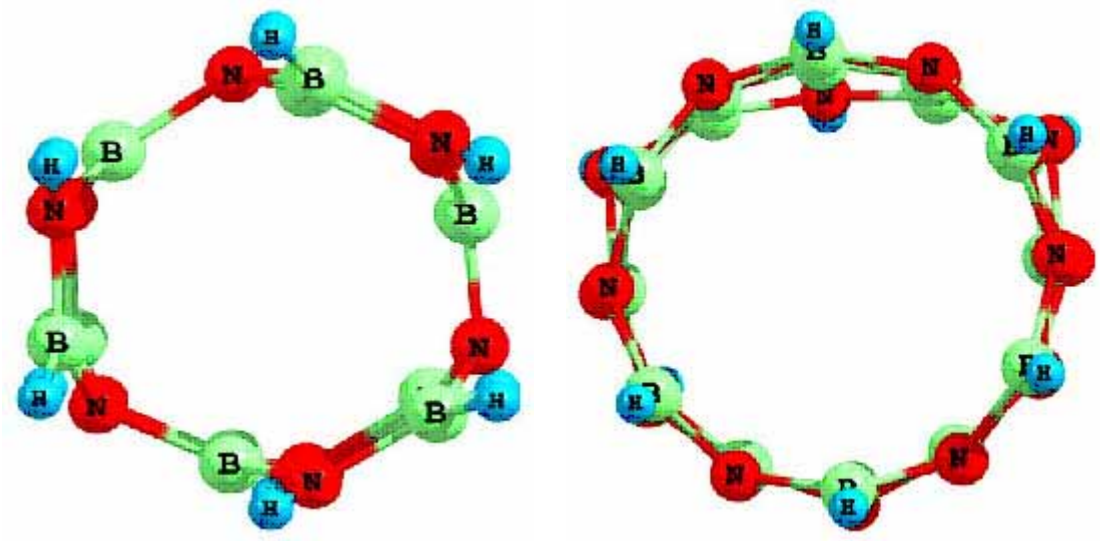

Fig. 5: Behind 2D views of the perfect in (3, 3) armchair and (6, 0) zigzag models of BNNTs

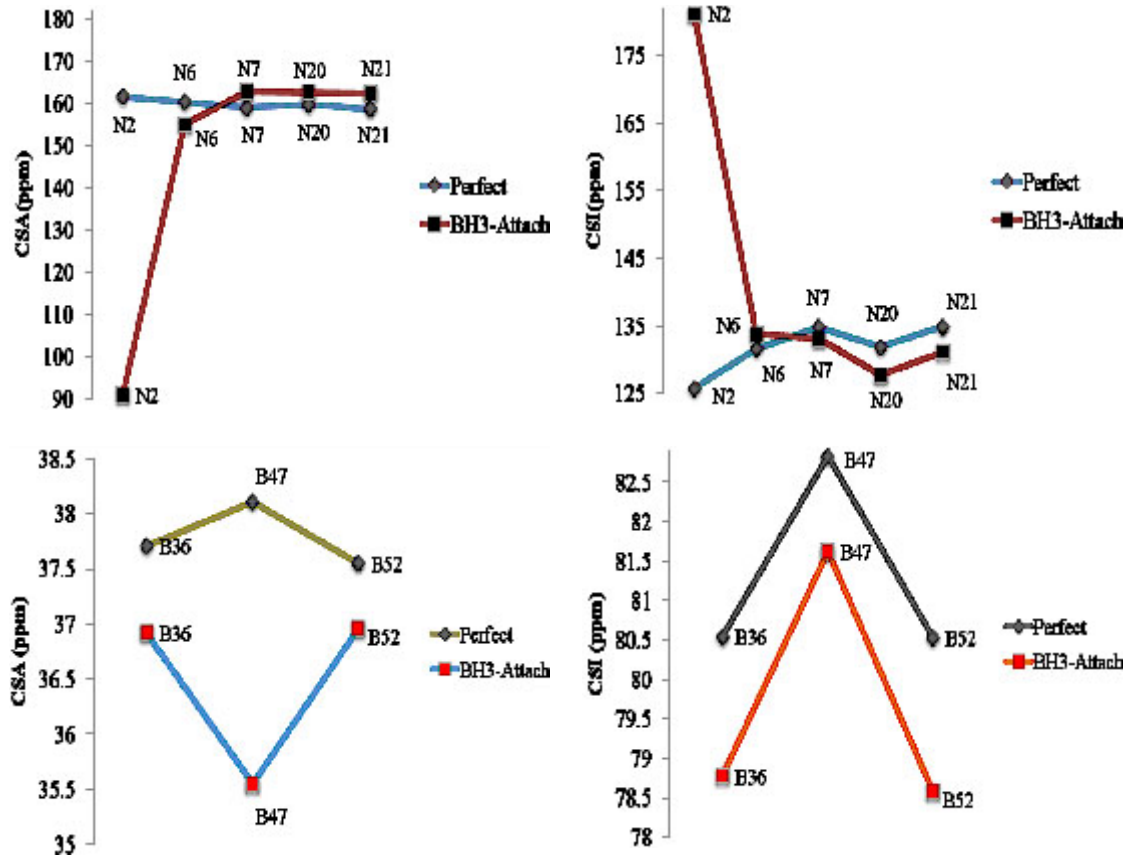

Fig. 6: Show compared results of various nucleus in perfect and BH_3-attach in (3, 3) armchair model of BNNTs

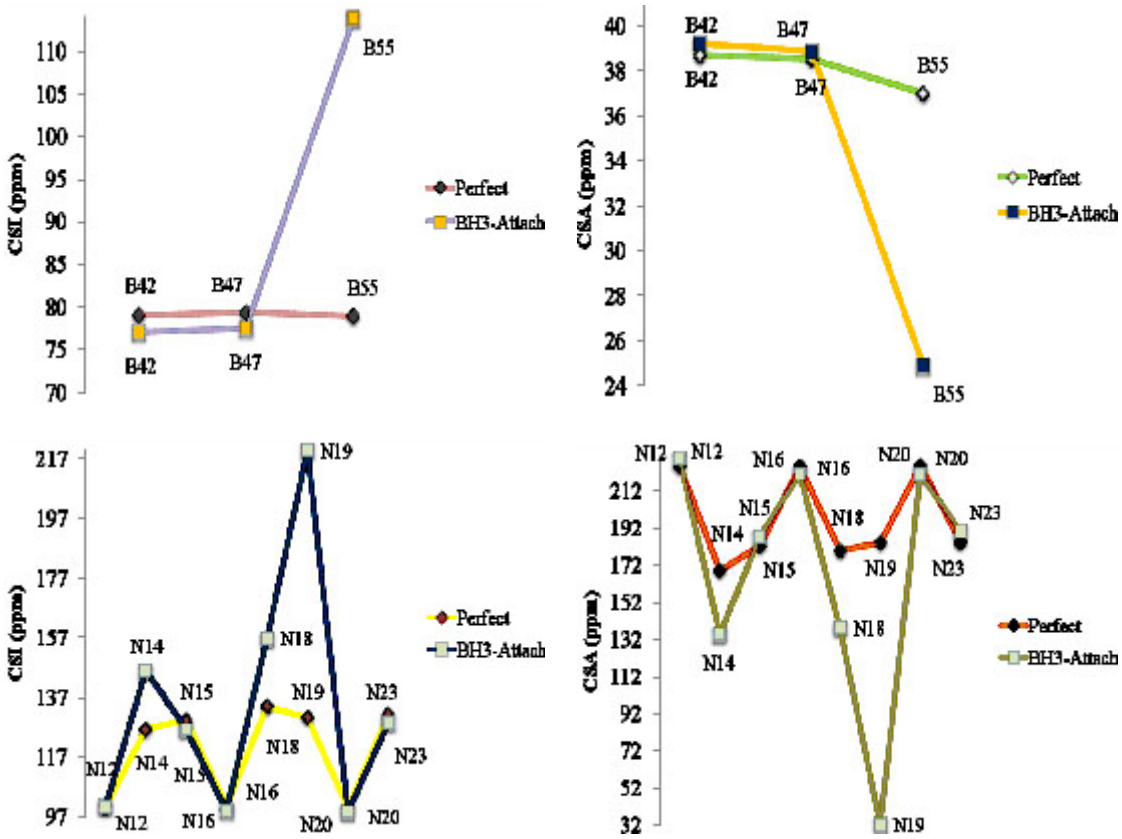

Fig. 7: Show compared results of various nucleus in perfect and BH_3-attach in (6, 0) zigzag model of BNNTs

Bond angle and dihedral angle in (6, 0) zigzag and (3, 3) armchair BNNTs

Investigation of bond and dihedral angles in armchair (*3, 3*) and zigzag (*6,* 0) BNNTs indicated that addition of BH_3 group to the surface of BNNTs did not significantly affect the values of bond and dihedral angles. Specific bonds, which were more affected by the added BH_3 group, were studied. The results were of subtle differences. The biggest changes were found among the studied angles in the zigzag form of which B42-N19-B55-N14 dihedral angle recorded the most significant change (166.4 °C to -6.9 °C). The results are reported in Tables 3 and 4.

NMR properties

The changes of the NMR parameter of these structures were calculated by GIAO method. The structures were optimized and NMR dependent parameters such as CS^I and CS^A were calculated. The results indicated that addition of BH_3 to the structure of BNNTs induced changes in the values of CS^I and CS^A parameters which affected the chemical properties of the nanotubes.

CS^I parameter

CS^I in armchair (3, 3) BNNTs in perfect and BH_3-attach

CS^I values indicated that addition of BH_3 group induced changes in CS^I parameter. The changes were in proportion with the position of BH_3 group on the surface of nanotube. Chemical shift of the nucleus of B, N, and H atoms were completely different. The results are reported in Table 5. In perfect state, the chemical shift of N nuclei had a 125 ppm to 144 ppm range and the chemical shift of B nuclei had a 78 ppm to 82 ppm range. The shift ranges

Table 1: Bond length (Angstrom) of perfect and BH_3-attach in (3, 3) armchair model of BNNTs.

Bond length	Armchair Perfect	Armchair BH_3 attach	Bond length	Armchair Perfect	Armchair BH_3 attach
N1-H23	1.011	1.011	N13-B39	1.471	1.472
N1-B34	1.420	1.418	N13-B41	1.448	1.447
N1-B35	1.461	1.460	N14-H24	1.011	1.011
N2-B36	1.458	1.496	N14-B40	1.420	1.419
N2-B47	1.465	1.504	N14-B41	1.461	1.460
N2-B52	1.453	1.509	N15-B43	1.448	1.446
N3-B35	1.465	1.463	N15-B48	1.466	1.466
N3-B36	1.458	1.451	N15-B54	1.471	1.473
N3-B51	1.453	1.448	N16-B43	1.465	1.466
N4-B34	1.471	1.474	N16-B45	1.458	1.459
N4-B37	1.448	1.448	N16-B46	1.453	1.451
N4-B51	1.466	1.462	N17-B41	1.465	1.467
N5-H30	1.011	1.010	N17-B42	1.453	1.450
N5-B47	1.461	1.458	N17-B45	1.458	1.457
N5-B53	1.420	1.410	N18-B35	1.448	1.449
N6-B49	1.448	1.448	N18-B40	1.471	1.472
N6-B52	1.466	1.452	N18-B42	1.466	1.462
N6-B53	1.471	1.480	N19-H32	1.011	1.011
N7-B50	1.452	1.455	N19-B43	1.461	1.462
N7-B51	1.462	1.469	N19-B44	1.420	1.416
N7-B52	1.462	1.448	N20-B44	1.471	1.477
N8-B37	1.465	1.465	N20-B46	1.466	1.463
N8-B38	1.453	1.453	N20-B47	1.448	1.434
N8-B50	1.458	1.455	N21-B36	1.452	1.439
N9-H26	1.011	1.011	N21-B42	1.462	1.469
N9-B37	1.461	1.460	N21-B46	1.462	1.459
N9-B39	1.420	1.420	H22-B40	1.195	1.195
N10-H29	1.011	1.011	H25-B39	1.195	1.195
N10-B49	1.461	1.459	H27-B34	1.195	1.195
N10-B54	1.420	1.419	H28-B53	1.195	1.194
N11-B48	1.453	1.453	H31-B44	1.195	1.193
N11-B49	1.465	1.462	H33-B54	1.195	1.195
N11-B50	1.458	1.455	B55-H56	-	1.206
N12-B38	1.462	1.463	B55-H57	-	1.208
N12-B45	1.452	1.450	B55-H58	-	1.199
N12-B48	1.462	1.462	N2-B55	-	1.803
N13-B38	1.466	1.465	-	-	-

were slightly affected by addition of a BH_3 group. After addition of a BH_3 group, the chemical shift of N nuclei had a 122 ppm to 181 ppm range and the chemical shift of B nuclei had a 78 ppm to 121 ppm range. Comparison of different nuclei showed that addition of a BH_3 group would increase the chemical shift range. Nuclei which were adjacent to the external BH_3 group showed the highest chemical shift. N2 and B47 had the highest chemical shift (Fig 6).

Table 2: Bond length (Angstrom) of perfect and BH_3-attach in (6, 0) zigzag model of BNNTs.

Bond length	Zigzag Perfect	Zigzag BH_3 attach	Bond length	Zigzag Perfect	Zigzag BH_3 attach
N1-B33	1.015	1.015	N14-B56	1.457	1.450
N1-B58	1.449	1.450	N15-B41	1.444	1.459
N1-B60	1.433	1.431	N15-B42	1.461	1.434
N2-B49	1.461	1.460	N15-B46	1.459	1.459
N2-B50	1.469	1.470	N16-B38	1.457	1.461
N2-B60	1.457	1.460	N16-B42	1.451	1.443
N3-B49	1.450	1.453	N16-B43	1.456	1.461
N3-B51	1.458	1.457	N17-H36	1.015	1.015
N3-B52	1.457	1.452	N17-B56	1.432	1.439
N4-B37	1.456	1.457	N17-B57	1.449	1.454
N4-B51	1.451	1.452	N18-B48	1.462	1.437
N4-B53	1.457	1.456	N18-B55	1.458	1.506
N5-H31	1.024	1.024	N18-B57	1.454	1.447
N5-B59	1.487	1.486	N19-B42	1.458	1.506
N5-B60	1.488	1.488	N19-B47	1.457	1.507
N6-B45	1.460	1.458	N19-B55	1.450	1.543
N6-B50	1.471	1.472	N20-B38	1.456	1.459
N6-B59	1.461	1.463	N20-B47	1.453	1.445
N7-B39	1.459	1.459	N20-B54	1.456	1.460
N7-B50	1.444	1.447	N21-H34	1.015	1.015
N7-B51	1.461	1.462	N21-B57	1.451	1.454
N8-B37	1.457	1.457	N21-B58	1.451	1.444
N8-B39	1.453	1.454	N22-B48	1.461	1.460
N8-B44	1.456	1.454	N22-B49	1.458	1.453
N9-H32	1.014	1.014	N22-B58	1.454	1.457
N9-B40	1.433	1.433	N23-B47	1.459	1.431
N9-B59	1.433	1.433	N23-B48	1.450	1.466
N10-B40	1.461	1.463	N23-B52	1.459	1.459
N10-B41	1.471	1.468	N24-B52	1.453	1.454
N10-B45	1.460	1.455	N24-B53	1.456	1.458
N11-B39	1.458	1.456	N24-B54	1.456	1.451
N11-B45	1.455	1.457	H25-B44	1.192	1.191
N11-B46	1.458	1.452	H26-B37	1.192	1.192
N12-B43	1.457	1.452	H27-B53	1.192	1.192
N12-B44	1.456	1.458	H28-B43	1.192	1.191
N12-B46	1.453	1.453	H29-B54	1.192	1.191
N13-H35	1.024	1.024	H30-B38	1.192	1.190
N13-B40	1.487	1.484	B61-N19	-	1.610
N13-B56	1.488	1.492	B61-H62	-	
N14-B41	1.469	1.446	B61-H63	-	1.197
N14-B55	1.460	1.507	B61-H64	-	1.196

Table 3: Bond Angle (Degree) and dihedral angle (Degree) of perfect and BH_3-attach in (3, 3) armchair model of BNNTs.

Bond Angle	Armchair Perfect	Armchair BH_3 attach
B52-N2-B55	-	105.4
B36-N2-B55	-	110.7
B47-N2-B55	-	106.1
B52-N2-N36	112.4	108.2
B36-N2-B47	119.2	117.2
B47-N2-B52	112.6	117.2
Dihedral Angle		
N7-B52-N2-B36	12.2	17.5
N7-B52-N2-B47	150.4	145.6
N6-B52-N2-B36	-149.9	-144.9
N6-B52-N2-B47	-11.6	-16.8
B55-N2-B52-N6	-	96.5
B55-N2-B52-N7	-	31.2
B55-N2-B36-N3	-	62.9
B55-N2-B36-N21	-	-135.3
B55-N2-B47-N20	-	137.9
B55-N2-B47-N5	-	59.9

Table 4:Bond Angle (Degree) and dihedral angle (Degree) of perfect and BH_3-attach in (6, 0) zigzag model of BNNTs.

Bond Angle	Zigzag Perfect	Zigzag BH_3 attach
B61-N19-B55	-	76.6
B61-N19-B47	-	118.6
B61-N19-B42	-	121.0
B42-N19-B55	117.5	117.2
B47-N19-B55	118.3	117.9
B42-N19-B47	110.0	104.3
Dihedral Angle		
B61-N19-B47-N23	-	108.3
B61-N19-B47-N20	-	-86.1
B61-N19-B42-N16	-	85.1
B61-N19-B42-N15	-	-110.2
B61-N19-B55-N18	-	-112.7
B61-N19-B55-N14	-	111.3
B42-N19-B55-N14	166.4	-6.9
B47-N19-B55-N18	11.7	2.8
B42-N19-B55-N18	147.9	128.9
B47-N19-B55-N14	-151.8	-133.0

CS^I in zigzag (6,0) BNNTs in perfect and BH_3-attach

Trends in chemical shift of some nuclei are compared in Table 6. Chemical shift of different nuclei in perfect state showed a 94 ppm to 100 ppm range in N nuclei and a 75 ppm to 81 ppm range in B nuclei (Table 6). However, by addition of a BH_3 group, the chemical shift of N nuclei changed to a 98 ppm to 219 ppm range and the chemical shift of B nuclei changed to a 73 ppm to 129 ppm range. Nuclei which were more affected by the BH_3 group were subjected to further investigation (Fig 7). CS^I values for the nuclei of different atoms showed that N19 and B55 recorded the highest shift range.

CS^A parameter

CS^A in armchair (3, 3) BNNTs in perfect and BH_3-attach

The result of CS^A values were the reverse of the results of CS^I values. In other words, as CS^I values increased CS^A values decreased. In perfect state, the chemical shift of N nuclei had a 114 ppm to 161 ppm range and the chemical shift of B nuclei at different parts of the nanotube had a 37 ppm to 55 ppm range. After addition of a BH_3 group, the chemical shift of N nuclei had a 91 ppm to 162 ppm range and the chemical shift of B nuclei had a 35 ppm to 56 ppm range. According to Figure 6 the nucleus of N2 and B47 atoms recorded the highest shift range after the addition of a BH_3 group.

CS^A in zigzag (6, 0) BNNTs in perfect and BH_3-attach

In perfect state, the chemical shift of N nuclei had a 74 ppm to 255 ppm range and the chemical shift of B nuclei had a 35 ppm to 52 ppm range. After addition of a BH_3 group, the chemical shift of N nuclei changed to a 32 ppm to 229 ppm range and the chemical shift of B nuclei changed to a 14 ppm to 53 ppm range. The nucleus of N19 and B55 atoms had the highest chemical shift range (Fig 7). It was evident that the addition of a BH_3 group to the surface of nanotube affected all CS^A values. The highest shifts were recorded in the nucleus of atoms directly affected by the BH_3 group.

Table 5: Isotropic Chemical Shift (ppm) and Anisotropic Chemical Shift (ppm) values for various nucleus of perfect and BH_3-attach in (3, 3) armchair model of BNNTs.

Armchair (3,3) BNNTs	Perfect		BH_3-Attach	
	CS^I	CS^A	CS^I	CS^A
N1	143.80	115.08	143.86	115.76
N2	125.72	161.67	181.18	91.04
N3	125.72	161.67	122.11	162.08
N4	131.56	160.37	132.14	158.77
N5	143.80	115.08	143.63	117.96
N6	131.56	160.37	133.77	155.10
N7	134.80	159.00	133.12	162.80
N8	125.37	161.50	126.34	161.62
N9	144.01	114.96	143.61	116.39
N10	144.01	114.96	144.63	114.67
N11	125.37	161.50	126.02	162.21
N12	135.09	159.07	134.19	158.72
N13	131.75	160.46	131.10	160.42
N14	143.87	115.05	143.88	115.53
N15	131.75	160.46	131.00	159.39
N16	125.36	161.60	126.50	161.37
N17	125.35	161.60	125.42	162.09
N18	131.88	159.74	131.98	162.01
N19	143.87	115.05	143.57	116.09
N20	131.88	159.74	127.69	162.66
N21	134.84	158.73	131.09	162.45
B34	78.97	55.57	79.04	55.89
B35	82.83	38.10	83.13	38.57
B36	80.54	37.71	78.78	36.92
B37	82.73	38.11	83.00	37.92
B38	80.46	37.65	80.45	37.95
B39	79.02	55.58	78.97	55.70
B40	78.95	55.62	78.91	55.44
B41	82.82	37.96	82.70	38.21
B42	80.46	37.86	80.93	37.13
B43	82.82	37.96	82.69	38.62
B44	78.96	55.62	78.95	55.75
B45	80.65	37.65	80.60	38.09
B46	80.46	37.86	81.87	36.23
B47	82.83	38.11	81.62	35.55
B48	80.46	37.65	80.51	38.01
B49	82.73	38.11	82.56	38.62
B50	80.56	37.89	80.74	37.92
B51	80.53	37.55	81.33	35.79
B52	80.53	37.55	78.58	36.96
B53	78.97	55.57	79.68	53.24
B54	79.02	55.58	78.92	56.08
B55	-	-	121.12	44.26

Table 6: Isotropic Chemical Shift (ppm) and Anisotropic Chemical Shift (ppm) values for various nucleus perfect and BH_3-attach in (6, 0) zigzag model of BNNTs.

Zigzag (6,0) BNNTs	Perfect		BH_3-Attach	
	CS^I	CS^A	CS^I	CS^A
N1	147.00	103.18	148.18	102.78
N2	126.37	169.36	125.43	167.57
N3	130.46	184.32	131.02	184.34
N4	100.53	225.51	99.70	224.81
N5	194.29	74.91	190.49	76.38
N6	123.55	176.22	122.62	174.97
N7	129.64	182.56	128.78	181.79
N8	100.31	225.60	99.31	225.18
N9	137.17	112.50	136.94	113.01
N10	123.58	176.15	126.62	178.57
N11	130.21	185.10	131.31	185.22
N12	100.32	225.62	100.44	229.25
N13	194.14	75.05	198.66	74.33
N14	126.36	169.32	146.16	134.95
N15	129.63	182.56	126.32	187.56
N16	100.54	225.52	99.20	221.67
N17	147.06	103.17	147.03	96.18
N18	134.06	180.11	156.75	138.39
N19	130.47	184.33	219.80	32.52
N20	100.24	225.85	98.76	221.35
N21	162.39	94.47	163.51	92.75
N22	134.09	180.10	137.22	179.94
N23	131.38	184.48	128.61	190.18
N24	100.24	225.85	100.24	229.43
B37	75.88	52.88	75.72	53.26
B38	75.96	52.83	73.81	53.13
B39	79.41	38.69	79.12	38.90
B40	75.49	43.88	75.29	42.95
B41	76.72	36.62	79.43	32.83
B42	79.06	38.70	77.06	39.23
B43	75.88	52.88	76.45	53.50
B44	76.05	52.89	75.98	52.42
B45	79.74	37.83	80.27	37.30
B46	79.41	38.69	80.49	38.59
B47	79.35	38.53	77.52	38.88
B48	78.56	35.99	81.49	36.40
B49	78.96	36.98	79.43	36.40
B50	76.71	36.63	75.95	37.20
B51	79.06	38.70	78.54	38.73
B52	79.35	38.53	80.43	38.39
B53	75.96	52.84	75.93	52.38
B54	76.01	52.78	76.59	53.31
B55	78.97	37.00	113.84	24.90
B56	75.71	43.16	75.21	42.91
B57	81.57	39.26	82.20	38.78
B58	81.57	39.25	82.14	38.40
B59	75.48	43.90	75.43	44.43
B60	75.70	43.17	75.56	43.78
B61	-	-	129.47	14.53

CONCLUSION

From the investigation of armchair (*3, 3*) and zigzag (*6,* 0) BNNTs under perfect and BH_3 attached states, it can be concluded that:

1. The values of CS^I and CS^A parameters have a regular trend in Boron nitride nanotubes under perfect state. Addition of a BH_3 group to the surface of nanotube affects this trend so that each parameter finds a specific value proportionate to the location of Boron, Hydrogen and Nitrogen nuclei.
2. The values of CS^I and CS^A parameters record their largest shift in the nucleus of the atoms directly linked to BH_3 groups.
3. Addition of a BH_3 group resulted in small changes in the values of bond length, bond angle, and dihedral angle. The changes were more significant in the area directly affected by BH_3.
4. Chemical shift of the nucleus of the BH_3 group, attached to the surface of the nanotube, shows different behavior in comparison with the chemical shift of the nucleus of B atom within the nanotube structure. The values of CS^I and CS^A parameters are usually higher in the nucleus of N atom in comparison with B atoms.

ACKNOWLEDGEMENTS

This work was supported by Islamic Azad University Shahre-rey branch and Islamic Azad University Mahshahr branch.

REFERENCES

1. M. Kawaguchi *et al. Journal of Physics and Chemistry of Solids,* **69**: 1171(2008).
2. M.S. Silberberg, *Chemistry: The Molecular Nature of Matter and Change* (5th ed.), New York: McGraw-Hill, (2009).
3. T.P. Crane, B.P. Cowan, *Physical Review B,* **62**: 11359 (2000).
4. R. Zedlitz, *Journal of Non-Crystalline Solids,* **403**: 198 (1996).
5. C.H. Henager, *Applied Optics,* **32**: 91 (1993).
6. S. Weissmantel, *Diamond and Related Materials,* **8** : 377 (1999).
7. G. Leichtfried *et al.* "13.5 Properties of diamond and cubic boron nitride". In P. Beiss et al. Landolt-Börnstein-Group VIII Advanced Materials and Technologies: Powder Metallurgy Data. Refractory, Hard and Intermetallic Materials. 2A2. Berlin: Springer. pp. 118 (2002).
8. J.H. Lan et al, *Physical Review B*, **79**: 115401(2009).
9. J. Hu, X. Ruan, Y.P. Chen, *Nano Letters,* **9**: 2730 (2009).
10. T. Ouyang, Y. Chen, Y. Xie, K. Yang, Z. Bao, J. Zhong. *Nanotechnology*, **21**: 245701(2010).
11. R. Haubner, M. Wilhelm, R. Weissenbacher, B. Lux, High Performance Non-Oxide Ceramics II, Series Structure and Bonding, vol. 102, Springer/Heidelberg, Berlin/New York, (2002).
12. P.B. Mirkarimi, K.F. McCarty, D.L. Medlin, Mater. *Sci. Eng.* R, **21**: 47 (1997).
13. X. Blase, A. Rubio, S.G. Louie, M.L. Cohen, *Europhys. Lett,* **28**: 335 (1994).
14. A. Loiseau, F. Willaime, N. Demoncy, G. Hug, H. Pascard, *Phys. Rev. Lett*, **76**: 4737 (1996).
15. E. Bengu, L.D. Marks, *Phys. Rev. Lett,* **86**: 2385 (2001).
16. V. Nirmala, P. Kolandaivel, *J. Mol. Struct. (THEOCHEM)*, **817**: 137 (2007).
17. A. Rubio, J.L. Corkill, L. Cohen, *Phys. Rev. B*, **49**: 5081 (1994).
18. N.G. Chopra, R.J. Luyken, K. Cherrey, H.C. Respi, M.L. Cohen, G. Louie, *Science*, **269**: 966 (1995).
19. T. Hirano, T. Oku, K. Suganuma, *Diamond Relat. Mater*, **9**: 625 (2000).
20. R. Ma, Y. Bando, T. Sato, *Chem. Phys. Lett*, **337**: 61 (2001).
21. W. Han, Y. Bando, K. Kurashima, T. Sato, *Appl. Phys. Lett,* **73**: 3085 (1998).
22. A. Rubio, Y. Miyamoto, X. Blasé, M.L. Cohen, S.G. Louie, *Phys. Rev. B*, **53**: 4023 (1996).
23. Z. Zhou, J. Zhao, Z. Chen, P.R. Schleyer, *J. Phys. Chem. B*, **110**: 25678 (2006).
24. E. Zahedi, A. Bodaghi, A. Seif, A,

Boshra, *Superlattices and Microstructures*, **49**: 169 (2011).
25. M.J. Frisch et al., GAUSSIAN 09. Gaussian, Inc., Pittsburgh, PA, (2010).
26. R.S. Drago, Physical Methods for Chemists, second ed, Saunders College Publishing, Florida, (1992).
27. U. Haeberlen, in: J.S. Waugh (Ed.), Advances in Magnetic Resonance, Academic Press, New York, (1976).
28. R. Dennington, T. Keith, J. Millam, K. Eppinnett, W.L. Hovell, R. Gilliland, GaussView, Version 3.07, Semichem, Inc., Shawnee Mission, KS, (2003).
29. K. Wolinski, J.F. Hinton, P. Pulay, *J. Am. Chem. Soc*, **112**: 8251 (1990).
30. F.J. London, *Phys. Radium*, **8**: 397 (1937).
31. R. Ditchfield, *Mol. Phys*, **27**: 789 (1974).